



Original Article

# CCNE1 Promotes the Progression of Hepatic Precancerous Lesion and the Malignant Phenotype of Hepatocellular Carcinoma



Kai Zhang<sup>1#</sup>, Xue Hu<sup>2#</sup>, Lichao Yao<sup>3</sup> and Wenzhi Guo<sup>1\*</sup>

<sup>1</sup>Department of Hepatobiliary and Pancreatic Surgery, the First Affiliated Hospital of Zhengzhou University, Zhengzhou, Henan, China; <sup>2</sup>Department of Oncology, General Hospital of Western Theater Command of PLA, Chengdu, Sichuan, China; <sup>3</sup>Department of Infectious Diseases, Renmin Hospital of Wuhan University, Wuhan, Hubei, China

Received: November 14, 2024 | Revised: March 16, 2025 | Accepted: April 07, 2025 | Published online: April 28, 2025

## Abstract

**Background and Aims:** The diagnosis of hepatic precancerous lesions (HPC) and early hepatocellular carcinoma (HCC) has significant public health implications and holds the potential to reduce the global burden of HCC. This study aimed to identify molecular features and biomarkers associated with HPC progression and early HCC development. **Methods:** RNA sequencing was used to identify differentially expressed genes in mouse HPC tissues and normal liver tissues. Cyclin E1 (CCNE1) expression in HPC tissues and HCC cells was assessed using immunohistochemistry, Western blotting, and real-time polymerase chain reaction. The effects of CCNE1 on HCC cell proliferation, migration, invasion, and apoptosis were evaluated using colony formation, wound healing, Transwell assays, and flow cytometry. The mechanism of CCNE1 was explored through Kyoto Encyclopedia of Genes and Genomes pathway analysis and gene set enrichment analysis and further validated through *in vitro* experiments. The interaction between CCNE1 and tumor-associated macrophages (TAMs) was investigated by co-culturing HCC cells with macrophages. **Results:** RNA sequencing and TCGA database analysis showed that CCNE1 expression was significantly elevated in mouse HPC tissues and human HCC samples and was associated with reduced survival rates. *In vitro* assays demonstrated that CCNE1 promoted HCC cell proliferation, migration, invasion, and survival by activating the PI3K/Akt signaling pathway. Additionally, CCNE1 induced TAM polarization toward the M2 phenotype by promoting the expression of CCL2 and CCL5 in HCC cells. **Conclusions:** CCNE1 promotes HPC progression and HCC cell proliferation, migration, invasion, and survival by activating the PI3K/Akt signaling pathway. Furthermore, CCNE1 enhances the secretion of CCL2 and CCL5 by HCC cells, promoting TAM infiltration and M2 polarization, thereby contributing to tumor progression.

**Keywords:** Hepatic precancerous lesion; Hepatocellular carcinoma; Malignant Phenotype, Cyclin E1; PI3K/Akt; Tumor-associated macrophages; Tumor immune microenvironment.

<sup>#</sup>Contributed equally to this work.

**\*Correspondence to:** Wenzhi Guo, Department of Hepatobiliary and Pancreatic Surgery, the First Affiliated Hospital of Zhengzhou University, Zhengzhou, Henan 450052, China. ORCID: <https://orcid.org/0000-0002-0821-1318>. Tel: +86-13838196990, E-mail: [fccguowz@zzu.edu.cn](mailto:fccguowz@zzu.edu.cn).

**Citation of this article:** Zhang K, Hu X, Yao L, Guo W. CCNE1 Promotes the Progression of Hepatic Precancerous Lesion and the Malignant Phenotype of Hepatocellular Carcinoma. J Clin Transl Hepatol 2025;13(7):555–567. doi: 10.14218/JCTH.2024.00428.

## Introduction

Hepatocellular carcinoma (HCC) is a significant global health concern, ranking as the sixth most common cancer and the second leading cause of cancer-related deaths worldwide.<sup>1</sup> Early-stage HCC is often asymptomatic, resulting in late diagnoses that limit access to curative treatments and lead to poor prognoses. HCC typically progresses in stages, beginning with hepatic precancerous lesions (HPC), which develop into dysplastic nodules, then into early HCC—characterized by small tumor masses lacking invasive features such as vascular infiltration or intrahepatic metastasis—and eventually into advanced HCC.<sup>2</sup> Identifying biomarkers for accurate early HCC diagnosis and understanding the mechanisms that drive HPC progression to invasive tumors are critical. These efforts may facilitate the prediction of HCC development from HPC and improve the standardization of histological diagnoses.

The immune system plays a dual role in both suppressing and promoting cancer. Tumors can evade immune surveillance by creating local or systemic immunosuppressive environments that hinder natural anti-tumor immunity and reduce the effectiveness of immunotherapy.<sup>3</sup> The tumor microenvironment (TME) is a dynamic and complex network composed of malignant cells, immune cells, and other factors influencing cancer progression and therapeutic responses.<sup>4</sup> Tumor-associated macrophages (TAMs), immune cells derived from the bone marrow, infiltrate the TME and may either inhibit or support tumor development. TAMs can enhance cancer cell proliferation, metastasis, and angiogenesis, while also suppressing anti-tumor immune responses. Depending on environmental cues, TAMs can polarize into either the anti-tumor M1 phenotype or the pro-tumor M2 phenotype.<sup>5,6</sup> In early neoplastic tumors, TAMs often exhibit an M1-like phenotype capable of eliminating some immunogenic tumor cells. However, as tumors progress, changes in the TME and macrophage function can lead to TAM polarization

toward the tumor-promoting M2-like phenotype.<sup>7</sup> Despite these findings, the role of TAMs in regulating the transition from HPC to HCC remains unclear.

E-type cyclins, including cyclins E1 and E2, are essential regulators of the cell cycle. They promote the transition from the G1 to the S phase by activating cyclin-dependent kinases (CDKs) and regulating DNA replication and centrosome biology.<sup>8</sup> Cyclin E1 (CCNE1) amplification or overexpression has been observed in multiple cancer types—including high-grade serous ovarian, endometrial, gastroesophageal, and breast cancers—and is often associated with poor prognosis.<sup>9–12</sup> In normal cells, CCNE1 levels are tightly regulated, peaking at the G1/S phase transition and decreasing as cells progress through the S phase. However, this regulation is frequently disrupted in cancer cells. Mechanisms such as CCNE1 gene amplification, disruption of the retinoblastoma/E2F pathway (which increases CCNE1 transcription), or mutations in the FBXW7 ubiquitin ligase (which impairs CCNE1 degradation) can lead to CCNE1 accumulation. Elevated CCNE1 levels can cause chromosomal and genetic instability, contributing to tumorigenesis.<sup>13,14</sup> Most HCCs reportedly overexpress E-type cyclins, promoting hepatocyte and HCC proliferation, even in a CDK2-independent manner.<sup>15</sup> Nevertheless, the specific role of CCNE1 in HPC development and its potential utility as an early diagnostic or prognostic biomarker, or as a therapeutic target in HCC, remain unclear.

This study explores the potential role of CCNE1 in HPC progression. The findings demonstrate that CCNE1 promotes HCC cell proliferation, migration, invasion, and survival via activation of the PI3K/Akt signaling pathway and by inducing pro-tumor M2 macrophage polarization through increased secretion of CCL2 and CCL5. These findings shed light on the oncogenic mechanisms of CCNE1 and its potential as an early biomarker for HCC progression in HPC, offering new avenues for HCC prevention and treatment strategies.

## Methods

### Animal experiments

Male C57BL/6 mice (four weeks old) were obtained from the Institute of Laboratory Animal Science, Chinese Academy of Medical Sciences (Beijing, China), and maintained in a pathogen-free animal facility. All mice had ad libitum access to standard rodent chow and filtered water. Thirty mice were randomly divided into two groups (15 mice per group) and treated as follows: the first group was injected intraperitoneally with 10% CCl<sub>4</sub> (1.0 mL/kg body weight, dissolved in corn oil) twice weekly for 24 weeks. The second group served as the control and received corn oil alone. Mice were sacrificed 24 h after the final CCl<sub>4</sub> injection, and serum and liver samples were collected for subsequent experiments. All procedures were approved by the Animal Care and Use Committee of The First Affiliated Hospital of Zhengzhou University (No. 2019-KY-21).

### Biochemical parameters

Serum levels of alanine transaminase and aspartate transaminase were measured using standard autoanalyzer methods on the Chemray 240 automatic biochemistry analyzer (Rayto, USA).

### Enzyme-linked immunosorbent assay (ELISA)

Serum alpha-fetoprotein (AFP) levels in mice and the concentrations of CCL2 and CCL5 secreted by HCC cells were determined using ELISA kits (Elabscience, China) according to the manufacturer's instructions.

### RNA-sequencing analysis

RNA sequencing was performed by BGI Tech Co., Ltd. (Shenzhen, China), using specific methods and procedures described previously.<sup>16</sup>

### Cell cultures

THP-1, HepG2, and Huh7 cell lines were purchased from the Shanghai Institute of Cell Biology, Chinese Academy of Sciences (Shanghai, China). THP-1 cells were maintained in RPMI-1640 medium (HyClone, USA), and HepG2 and Huh7 cells were maintained in DMEM (HyClone, USA) supplemented with 10% fetal bovine serum (Gibco, USA) and 100 U/mL penicillin-streptomycin (Beyotime, China) at 37°C in a 5% CO<sub>2</sub> incubator. The medium was changed every two to three days. THP-1 cells were treated with 100 ng/mL PMA (MedChemExpress, USA) for 24 h to generate non-polarized (M0) macrophages.

### Histopathology

Liver tissue samples were fixed in 4% paraformaldehyde, embedded in paraffin, sectioned at 5 μm, and stained with hematoxylin and eosin for general histopathological evaluation. Detailed experimental methods are described previously.<sup>17</sup>

### Immunohistochemistry

Paraffin-embedded tissue samples were sectioned at 5 μm, deparaffinized, and rehydrated. Sections were incubated overnight at 4°C with primary antibodies against AFP (1:100, ab46799, Abcam), vascular endothelial growth factor (VEGF) (1:100, ab27278, Abcam), and F4/80 (1:100, ab300421, Abcam). Detailed methods are described previously.<sup>17</sup>

### siRNA transfection

HepG2 and Huh7 cells were seeded in 6-well plates and incubated for 24 h. At 50% confluency, cells were transfected with CCNE1-specific siRNA using Lipofectamine™ 2000 (Invitrogen, USA) in Opti-MEM. Detailed methods are described previously.<sup>18</sup>

### Cell viability assay

Cell viability was assessed using the Cell Counting Kit-8 according to the manufacturer's instructions. Briefly, 2,000 cells per well were seeded in 96-well plates and cultured for 12, 24, 48, and 72 h. Cell Counting Kit-8 solution was added, and absorbance at 450 nm was measured using a microplate reader.

### Colony formation assay

HCC cells were seeded in six-well plates and cultured for 10 days. Colonies were fixed with 4% paraformaldehyde and stained with 0.1% crystal violet for 30 m. Detailed methods are described previously.<sup>19</sup>

### Wound-healing assay

HCC cells were seeded in six-well plates and grown to 80% confluence. A scratch was made, and images were captured at 0 and 48 h using an inverted microscope. Detailed methods are described previously.<sup>19</sup>

### Transwell invasion assay

To assess cell invasiveness, the upper chamber of the transwell insert was pre-coated with Matrigel (Corning, NY, USA). Cells were seeded in the upper chamber, and migrated cells

**Table 1. Primer sequences used for RT-qPCR**

Mouse	
Ccne1	Forward sequence: 5'-CTCCCACAACATCCAGACCC-3'
	Reverse sequence: 5'-AGCAACCTACAACACCCGAG-3'
Human	
CD86	Forward sequence: 5'-CAGGGACTAGCACAGACACAC-3'
	Reverse sequence: 5'-CAGGTTGACTGAAGTTAGCAGAG-3'
iNOS	Forward sequence: 5'-CGTGGAGACGGAAAGAAGT-3'
	Reverse sequence: 5'-GACCCCAGGCAAGATTTGGA-3'
CD206	Forward sequence: 5'-GGGAAAGGTTACCCCTGGTGG-3'
	Reverse sequence: 5'-GTCAAGGAAGGGTCGGATCG-3'
Arg1	Forward sequence: 5'-TTAAGAACAAGAGTGTGATGTGAA-3'
	Reverse sequence: 5'-TCCAATTGCCAACTGTGGT-3'
CCL2	Forward sequence: 5'-AGCAGCAAGTGTCCCAAAGA-3'
	Reverse sequence: 5'-GGTGTCTGGGAAAGCTAGG-3'
CCL5	Forward sequence: 5'-GACAGCAAGTCTGGCAGGAT-3'
	Reverse sequence: 5'-TTTTGACAAAGCAGCGCCTC-3'

RT-qPCR, Real-time polymerase chain reaction; Ccne1, Cyclin E1; iNOS, Inducible nitric oxide synthase; Arg1, Arginase 1; CCL2, Chemokine (C-C motif) ligand 2; CCL5, Chemokine (C-C motif) ligand 5.

were counted and imaged in three randomly selected fields. Detailed methods are described previously.<sup>19</sup>

#### Flow cytometry

HCC cells were washed with cold PBS, resuspended in binding buffer, and stained with Annexin V-FITC and propidium iodide for 20 m at room temperature. Apoptosis was analyzed using flow cytometry. Detailed methods are described previously.<sup>19</sup>

#### Real-time polymerase chain reaction (RT-qPCR)

Total RNA was extracted using TRIzol (Beyotime, China). cDNA was synthesized from 2 µg of total RNA using the BeyoRT™ Reagent Kit (Beyotime, China). mRNA expression levels were determined using specific primers and analyzed using the 2<sup>-ΔΔCt</sup> method, normalized to GAPDH expression. Detailed methods are described previously.<sup>19</sup> Primer sequences are listed in Table 1.

#### Western blotting

Total protein was extracted using RIPA lysis buffer. Detailed methods are described previously.<sup>19</sup> Primary antibodies included: AFP (1:1,000, ab284388, Abcam), VEGF (1:1,000, ab27278, Abcam), CCNE1 (1:1,000, ab211342, Abcam), MMP2 (1:1,000, A19080, ABclonal), MMP9 (1:1,000, A2095, ABclonal), Cleaved Caspase-3 (1:1,000, A22869, ABclonal), Bax (1:1,000, A19684, ABclonal), Bcl-2 (1:1,000, A0208, ABclonal), PI3K (1:1,000, ab302958, Abcam), p-PI3K (1:1,000, ab278545, Abcam), Akt (1:1,000, ab8805, Abcam), p-Akt (1:1,000, ab38449, Abcam), CD206 (1:1,000, ab64693, Abcam), Arg-1 (1:1,000, ab133543, Abcam), CCL2 (1:1,000, A7277, ABclonal), CCL5 (1:1,000, A5630, ABclonal), and GAPDH (1:3,000, AC001, ABclonal).

#### Statistical analysis

Data analysis was conducted using GraphPad Prism 8.0 (GraphPad Software, USA). Bar graphs represent the mean

± standard deviation. Statistical significance was determined using one-way ANOVA or a two-tailed unpaired Student's *t*-test. A *P* < 0.05 was considered statistically significant.

## Results

### General conditions and histopathological changes in mice with hepatic precancerous lesions

Mice in the control group exhibited normal behavior, alertness, good energy, and clean fur. In contrast, mice in the model group showed signs of poor general condition, lethargy, reduced activity and appetite, and thinning hair. The model group also exhibited decreased liver weight (Fig. 1A), an increased liver-to-body weight ratio (Fig. 1B), and elevated serum alanine transaminase, aspartate transaminase, and AFP levels (Fig. 1C–E). Gross examination of liver morphology revealed a rough, firm texture and dull coloration in the model group. Hematoxylin and eosin staining showed disrupted hepatic lobular architecture, disorganized hepatocyte cords, and numerous heterocellular clusters characterized by hyperchromatic nuclei, increased nuclear-to-cytoplasmic ratios, basophilic cytoplasm, and infiltration of inflammatory cells. Masson staining revealed a marked increase in hepatic fibrotic deposition in the HPC group compared to the control group (Fig. 1F). Additionally, immunohistochemistry (Fig. 1G) and Western blotting (Fig. 1H) demonstrated significantly increased expression of AFP and VEGF in the HPC group relative to the control group.

### CCNE1 is highly expressed in the liver tissues of mice with hepatic precancerous lesions

RNA sequencing was conducted on liver tissues from the control and HPC groups to elucidate molecular mechanisms underlying HPC development. Unsupervised hierarchical clustering and principal component analysis clearly distinguished liver samples from control and model mice into two distinct clusters, indicating significant molecular dif-

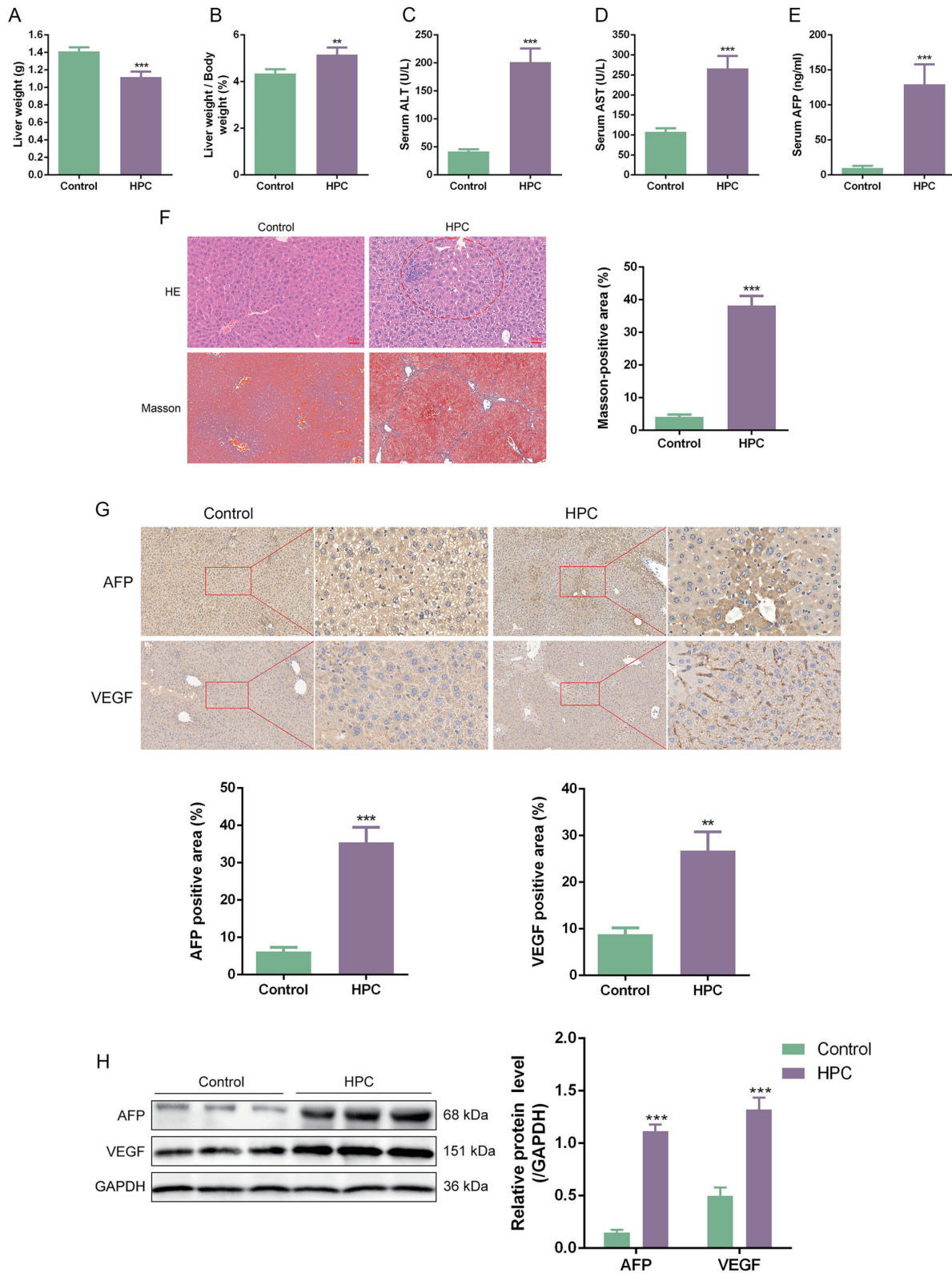


**Fig. 1. General conditions and histopathological changes in mice with hepatic precancerous lesions.** (A) Liver weight of mice. (B) Liver-to-body weight ratio. (C-E) Serum levels of ALT, AST and AFP. (F) Representative H&E and Masson-stained images; scale bar: 50  $\mu$ m. (G) Immunohistochemistry for AFP and VEGF; scale bar: 20  $\mu$ m. (H) Protein levels of AFP and VEGF.  $**p < 0.01$ ;  $***p < 0.001$ . HPC, Hepatic precancerous lesions; ALT, alanine aminotransferase; AST, Aspartate aminotransferase; AFP, Alpha fetoprotein; VEGF, Vascular endothelial growth factor; GAPDH, glyceraldehyde 3-phosphate dehydrogenase.

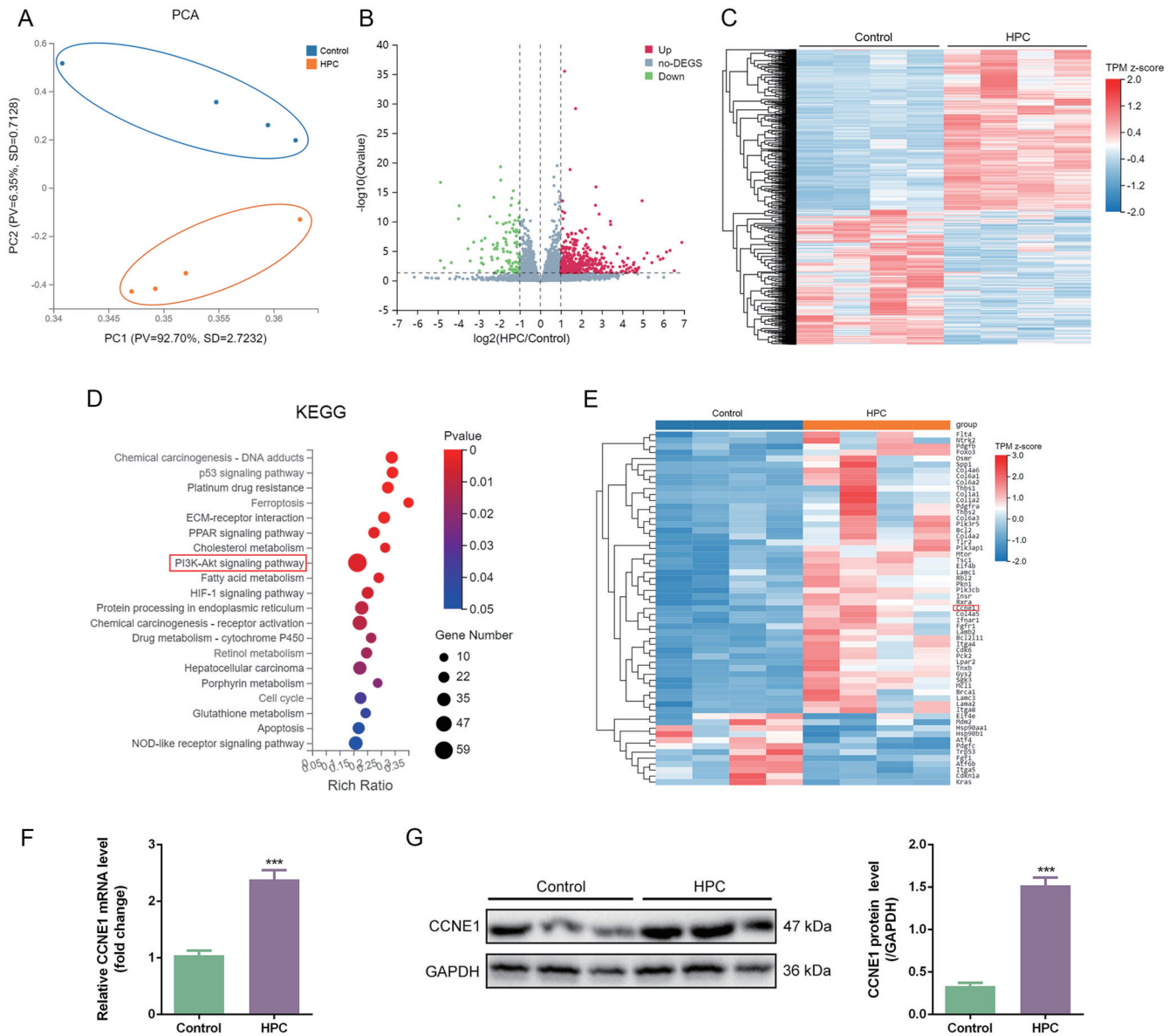


**Fig. 2. Expression levels of CCNE1 in liver tissues of mice with hepatic precancerous lesions.** (A) PCA of RNA-seq data. (B) Volcano plot of DEGs. (C) Heatmap of DEGs. (D) KEGG pathway enrichment analysis of DEGs. (E) Heatmap of DEGs involved in the PI3K/Akt signaling pathway. (F) mRNA expression level of CCNE1. (G) Protein expression level of CCNE1. \*\*\* $p < 0.001$ . HPC, Hepatic precancerous lesions; CCNE1, Cyclin E1; GAPDH, glyceraldehyde 3-phosphate dehydrogenase.

ferences (Fig. 2A). A total of 2,038 differentially expressed genes (DEGs) were identified, with 1,105 upregulated and 933 downregulated genes (Fig. 2B–C). The Kyoto Encyclopedia of Genes and Genomes pathway enrichment analysis showed that the DEGs were primarily involved in the p53 signaling pathway, extracellular matrix–receptor interaction, PPAR signaling, fatty acid metabolism, PI3K/Akt signaling, and NOD-like receptor signaling pathways (Fig. 2D). The PI3K/Akt pathway, which is crucial in various cancers, regulates cancer cell survival, metastasis, metabolism, and also modulates the TME, including angiogenesis and recruitment of inflammatory mediators.<sup>20</sup> Among 59 DEGs in this pathway, CCNE1 was among the top 10 genes with the highest fold changes, alongside THBS1, Col1a2, Col1a1, Col4a6, CDKN1A, NTRK2, Col6a2, LPAR2, and Col6a1 (Fig. 2E). RT-

qPCR (Fig. 2F) and Western blotting (Fig. 2G) confirmed significant upregulation of CCNE1 mRNA and protein levels in the HPC group compared to the control group.

**CCNE1 is involved in the progression from HPC to HCC**

Comprehensive analysis of HCC RNA sequencing data from the TCGA database showed a significant increase in CCNE1 expression in human HCC tissues (Fig. 3A). Stratified analysis by tumor stage revealed that CCNE1 expression was significantly higher in intermediate/advanced HCC compared to early-stage HCC (Fig. 3B). In early-stage HCC (BCLC 0/A), CCNE1 levels positively correlated with tumor size and risk of vascular invasion. In advanced-stage HCC (BCLC C/D), higher CCNE1 expression was significantly associated with distant metastasis (Table 2), suggesting that CCNE1 may be in-

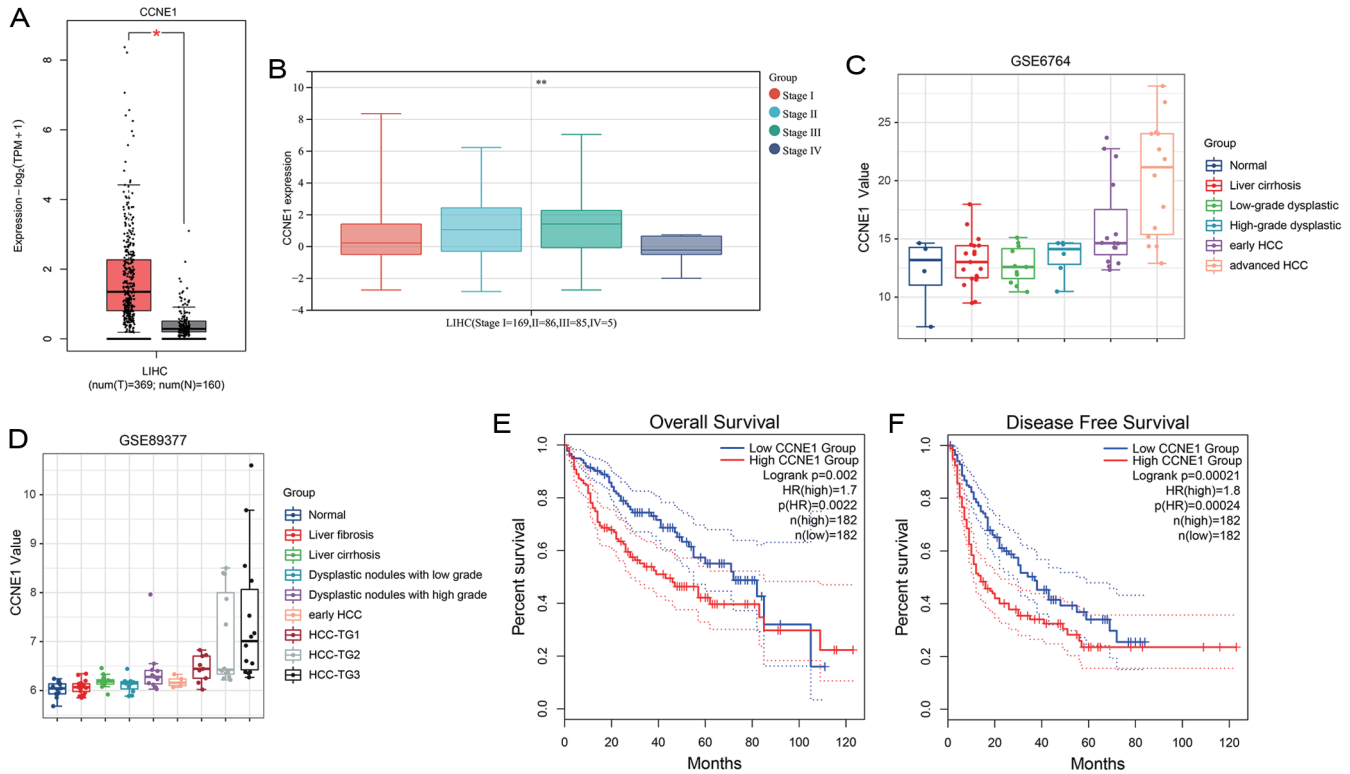


**Fig. 3. Role of CCNE1 in the progression from HPC to HCC.** (A) CCNE1 expression in human normal liver and HCC samples. (B) CCNE1 expression across various HCC stages (TCGA database). (C-D) CCNE1 expression during malignant transition from HPC to advanced HCC (GEO database). (E-F) Relationship between CCNE1 expression and patient survival. \**p* < 0.05; \*\**p* < 0.01. CCNE1, Cyclin E1; HCC, Hepatocellular carcinoma.

**Table 2. Correlation between CCNE1 expression and clinical features in HCC**

Group	Clinical Feature	Sample Distribution	FPKM (Median ± IQR)	P-value
Early-stage HCC (BCLC 0/A)	Gender	Male: 80	2.5 ± 1.2	0.45
		Female: 40	2.3 ± 1.0	
	Age (years)	≤60: 70	2.4 ± 1.1	0.78
		>60: 50	2.6 ± 1.3	
	Tumor Size	≤5 cm: 85	2.1 ± 0.9	0.04*
		>5 cm: 35	3.0 ± 1.6	
Liver cirrhosis	Yes: 90	2.5 ± 1.3	0.15	
	No: 30	2.2 ± 1.0		
Vascular Invasion	Positive: 30	3.2 ± 1.5	0.02*	
	Negative: 90	1.8 ± 0.9		
Advanced-stage HCC (BCLC C/D)	Gender	Male: 50	3.8 ± 1.8	0.62
		Female: 30	3.5 ± 1.6	
	Age (years)	≤60: 40	3.6 ± 1.7	0.91
		>60: 40	3.7 ± 1.9	
	Tumor Size	≤5 cm: 45	3.2 ± 1.5	0.08
		>5 cm: 35	4.0 ± 2.0	
Liver cirrhosis	Yes: 70	3.7 ± 1.8	0.27	
	No: 10	3.1 ± 1.4		
Distant Metastasis	Positive: 25	4.5 ± 2.1	0.003**	
	Negative: 55	2.3 ± 1.2		

\**p* < 0.05; \*\**p* < 0.01. CCNE1, Cyclin E1; HCC, Hepatocellular carcinoma; FPKM, Fragments Per Kilobase of exon model per Million mapped fragments; BCLC, Barcelona Clinic Liver Cancer.

involved in tumor progression. Furthermore, analysis of clinical datasets representing stages of progression from HPC to HCC (GSE6764, GSE89377) demonstrated that CCNE1 expression was significantly elevated in HPC samples compared to normal liver tissue, with a gradual increase during the transition to HCC (Fig. 3C–D). Kaplan–Meier survival analysis showed that high CCNE1 expression was significantly associated with reduced overall survival (Fig. 3E–F). These findings support a pivotal role for CCNE1 in the early malignant transformation of HCC.

#### **Knockdown of CCNE1 inhibits HCC cell proliferation, migration, and invasion and promotes apoptosis**

To investigate the role of CCNE1 in HCC progression, its expression was analyzed in various HCC cell lines, including SMMC-7721, SNU-449, Huh7, HepG2, and Hep3B. All showed significantly higher CCNE1 expression compared to normal hepatocyte cell lines (L02) (Fig. 4A). HepG2 and Huh7 cells, which had the highest CCNE1 expression levels, were selected for further experiments. Using siRNA to knockdown CCNE1, a marked reduction in HCC cell viability (Fig. 4B–C) and colony formation (Fig. 4D) was observed in the siCCNE1 group compared to controls. Wound-healing (Fig. 4E–F) and Transwell assays (Fig. 4G–H) showed that CCNE1 knockdown significantly inhibited cell migration and invasion. Western blotting showed reduced expression of MMP2 and MMP9, which are critical mediators of tumor invasion (Fig. 4J–K). Flow cytometry analysis revealed increased apoptosis in the siCCNE1 group (Fig. 4I), corroborated by elevated levels of Cleaved Caspase-3 and Bax, and reduced Bcl-2 expression (Fig. 4J–K). These results indicate that CCNE1 can promote HCC cell proliferation, migration, invasion, and survival.

#### **CCNE1 promotes HCC progression by activating the PI3K/Akt signaling pathway**

Gene set enrichment analysis (GSEA) of RNA sequencing data revealed that the PI3K/Akt signaling pathway was upregulated in the HPC group (Fig. 5A). This finding was confirmed by Western blotting, which showed increased levels of p-PI3K and p-Akt in the HPC group compared to the control group (Fig. 5B), indicating activation of the PI3K/Akt pathway during HPC development. Further investigation into the role of the PI3K/Akt pathway in HCC progression showed that CCNE1 knockdown reduced the phosphorylation levels of PI3K and Akt (Fig. 5C–D). To validate the role of the PI3K/Akt pathway, LY294002 (a PI3K inhibitor) or 740Y-P (a PI3K activator) was added to the cell culture medium. Functional assays including colony formation (Fig. 5E), wound healing (Fig. 5F–H), Transwell migration/invasion (Fig. 5G–I), and flow cytometry (Fig. 5J) demonstrated that inhibition of the PI3K/Akt pathway reversed the oncogenic effects of CCNE1 on HCC cell proliferation, migration, invasion, and survival. Interestingly, activation of the PI3K/Akt pathway did not significantly rescue the phenotype of HCC cells in the siCCNE1 groups, suggesting that CCNE1 acts upstream of PI3K/Akt. These findings indicate that CCNE1 promotes the malignant phenotype of HCC cells by activating the PI3K/Akt signaling pathway, underscoring its critical role in HCC progression.

#### **CCNE1 promotes M2 macrophage polarization in HCC**

Circulating bone marrow-derived monocytes migrate to the tumor site and differentiate into TAMs under the influence of cytokines and chemokines in TME.<sup>21</sup> TAM plays a critical role in tumorigenesis by promoting tumor cell proliferation, invasion, angiogenesis, and metastasis.<sup>22</sup> The Gene Ontology

and GSEA of RNA sequencing data identified several pathways associated with HPC development, including “cytokine receptor activity,” “inflammatory response,” and “monocyte chemotaxis” (Fig. 6A). Additionally, analysis using the Tumor Immune Estimation Resource revealed that CCNE1 expression in HCC positively correlated with immune cell infiltration, including B cells, CD8<sup>+</sup> T cells, CD4<sup>+</sup> T cells, and macrophages (Fig. 6B). Immunohistochemistry further confirmed increased macrophage infiltration and neovascularization in liver tissues of HPC mice compared to controls (Figs. 1G, 6C). *In vitro* co-culture of HCC cells with PMA-induced THP-1 monocytes showed that HCC cells elevated the mRNA and protein levels of M2 polarization markers (CD206 and Arg-1) in THP-1-derived macrophages after 48 h (Fig. 6D–G). However, CCNE1 knockdown via siRNA reduced CD206 and Arg-1 expression while increasing mRNA levels of M1 markers (CD86 and iNOS). Moreover, TAMs derived from PMA-induced THP-1 cells and co-cultured with HCC cells promoted VEGF expression in HepG2 and Huh7 cells, an effect that was reversed by CCNE1 silencing (Fig. 6H–I). These findings suggest that CCNE1 overexpression promotes TAM polarization toward the tumor-promoting M2 phenotype, thereby enhancing angiogenesis and metastasis in HCC.

#### **CCNE1 induces TAM polarization by promoting CCL2 and CCL5 expressions**

To further elucidate the mechanism by which CCNE1 drives TAM polarization, we focused on chemokines in the TME, which regulate immune cell migration and influence tumor immune composition and therapy resistance.<sup>23,24</sup> RNA sequencing analysis showed that CCR1, CCL5, CCL2, and CCR2 were enriched in the “monocyte chemotaxis” pathway and were significantly upregulated in the HPC group ( $\log_2FC > 1$ , adjusted  $P < 0.05$ ) (Fig. 7A). ELISA, RT-qPCR, and Western blotting revealed that CCNE1 silencing significantly reduced CCL2 and CCL5 expression in HCC cells (Fig. 7B–E). To test the functional relevance, neutralizing antibodies (NAbs) against CCL2 and CCL5 were added to a co-culture system of HCC cells and PMA-induced THP-1 macrophages. Both CCL2-NAb and CCL5-NAb partially attenuated TAM polarization induced by HCC cells, while the combination of both completely blocked the polarization effect (Fig. 7F–I). These findings suggest that CCNE1 promotes TAM polarization in HCC via a CCL2/CCL5-dependent mechanism.

#### **Discussion**

Precancerous lesions are tissues with a high risk of tumorigenesis due to DNA damage, genomic instability, and inflammation.<sup>25</sup> HCC develops through a stepwise process from precancerous lesions, including low-grade and high-grade dysplastic nodules, to advanced cancer.<sup>2</sup> Early detection of small HCC or precancerous lesions is crucial for optimal treatment; however, the molecular changes associated with HPC progression and its morphological and molecular features are not fully understood. Hence, identifying molecular markers of early HCC progression in HPC is essential for early detection and treatment. The present study not only elucidates the oncogenic mechanisms of CCNE1 in HCC but also underscores its pivotal role as a molecular bridge linking HPC to invasive HCC. Our findings reveal that CCNE1 overexpression is an early event in hepatocarcinogenesis, detectable in HPC tissues and progressively amplified during malignant transformation. This spatiotemporal expression pattern positions CCNE1 as a potential biomarker for early diagnosis (e.g., via liquid biopsy) and risk stratification to guide surveillance protocols.

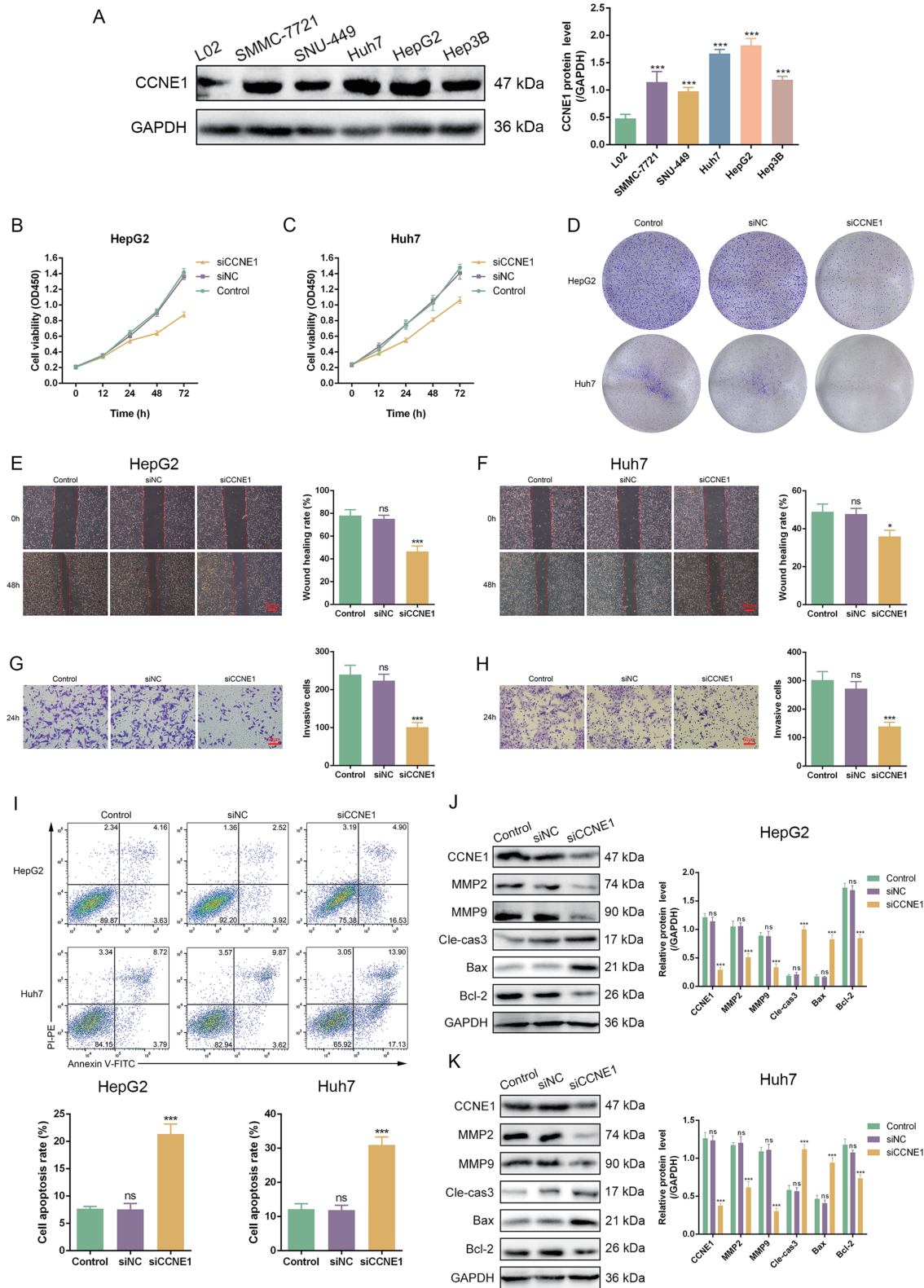


**Fig. 4. Effect of CCNE1 on the malignant phenotype of HCC cells.** (A) Protein level of CCNE1. (B-C) Cell viability in HepG2 and Huh7. (D) Cell proliferation in HepG2 and Huh7. (E-F) Cell migration in HepG2 and Huh7. (G-H) Cell invasion in HepG2 and Huh7. (I) Cell apoptosis in HepG2 and Huh7. (J-K) Protein levels of CCNE1, MMP2, MMP9, Cleaved Caspase-3, Bax, and Bcl-2. ns, not significant; \* $p < 0.05$ ; \*\*\* $p < 0.001$ . CCNE1, Cyclin E1; MMP2, Matrix metalloproteinase 2; MMP9, Matrix metalloproteinase 9; GAPDH, glyceraldehyde 3-phosphate dehydrogenase.

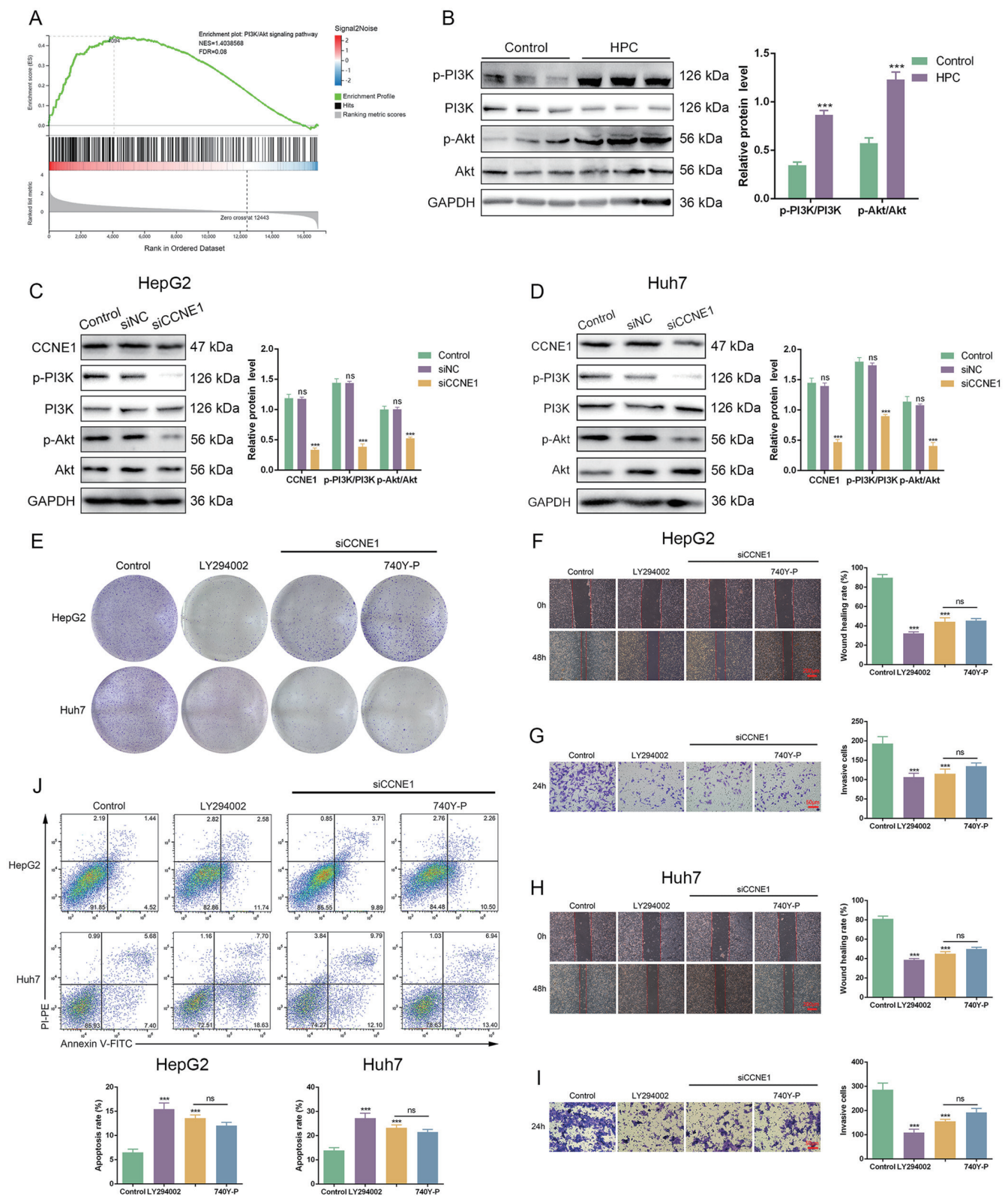


**Fig. 5. Effect of CCNE1 on the PI3K/Akt signaling pathway.** (A) GSEA analysis of RNA-seq data. (B) Protein levels of p-PI3K, PI3K, p-Akt, and Akt in liver tissues. (C-D) Protein levels of CCNE1, p-PI3K, PI3K, p-Akt, and Akt in HepG2 and Huh7 cells. (E) Cell proliferation in HepG2 and Huh7 cells. (F) Cell migration in HepG2. (G) Cell invasion in HepG2. (H) Cell migration in Huh7. (I) Cell invasion in Huh7. (J) Cell apoptosis in HepG2 and Huh7. ns, not significant; \*\*\* $p < 0.001$ . HPC, Hepatic precancerous lesions; PI3K, Phosphatidylinositol 3-kinase; Akt, Protein kinase B; CCNE1, Cyclin E1; GAPDH, glyceraldehyde 3-phosphate dehydrogenase.

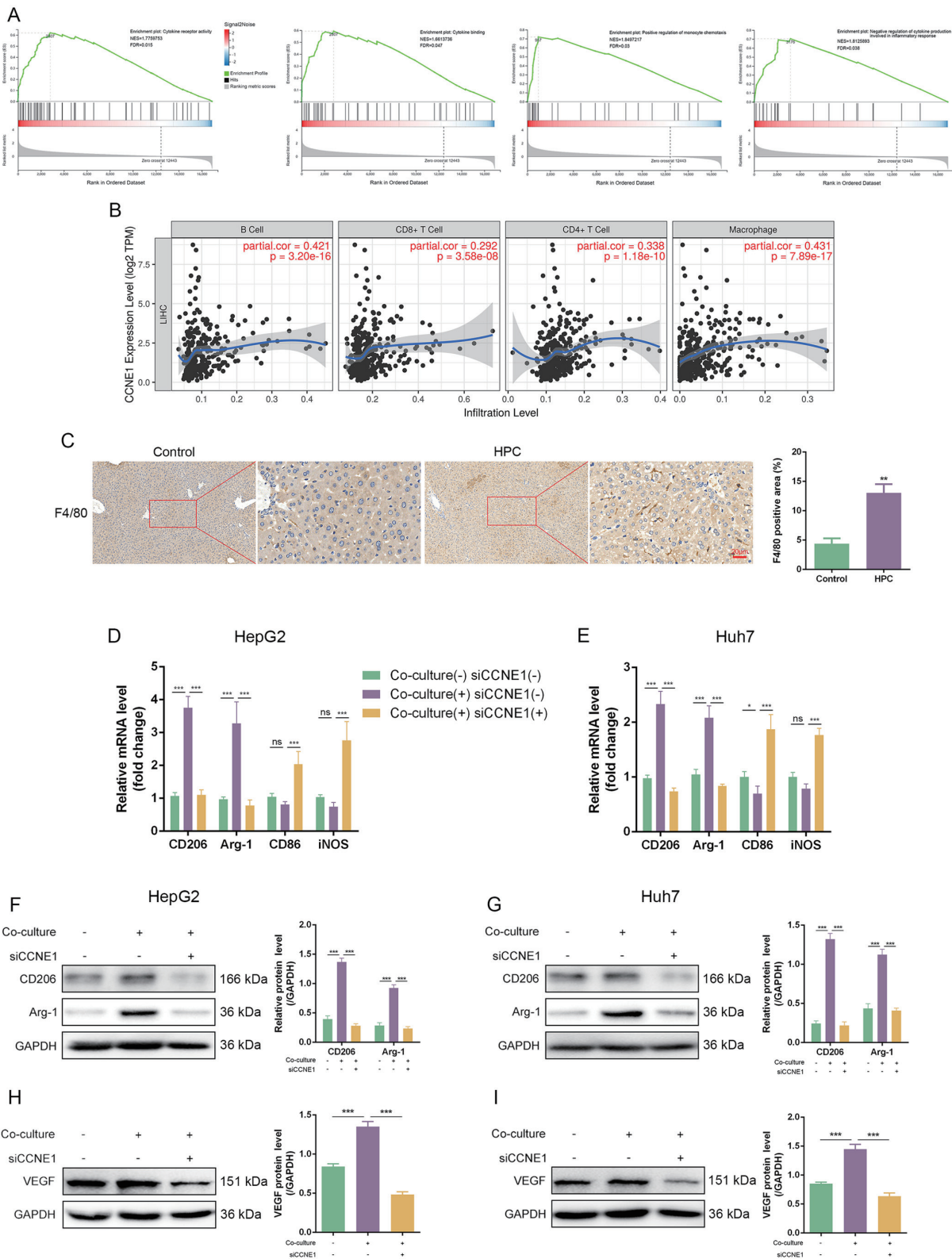


**Fig. 6. Effect of CCNE1 on macrophage polarization.** (A) GSEA analysis of RNA-seq data. (B) Correlation between CCNE1 expression and immune cell infiltration. (C) Immunohistochemical staining for F4/80; scale bar: 20  $\mu$ m. (D-E) mRNA levels of CD206, Arg-1, CD86, and iNOS. (F-G) Protein levels of CD206 and Arg-1. (H-I) Protein levels of VEGF. ns, not significant; \* $p < 0.05$ ; \*\*\* $p < 0.001$ . HPC, Hepatic precancerous lesions; Arg-1, Arginase-1; iNOS, Inducible nitric oxide synthase; VEGF, Vascular endothelial growth factor; GAPDH, glyceraldehyde 3-phosphate dehydrogenase; +, with; -, without.

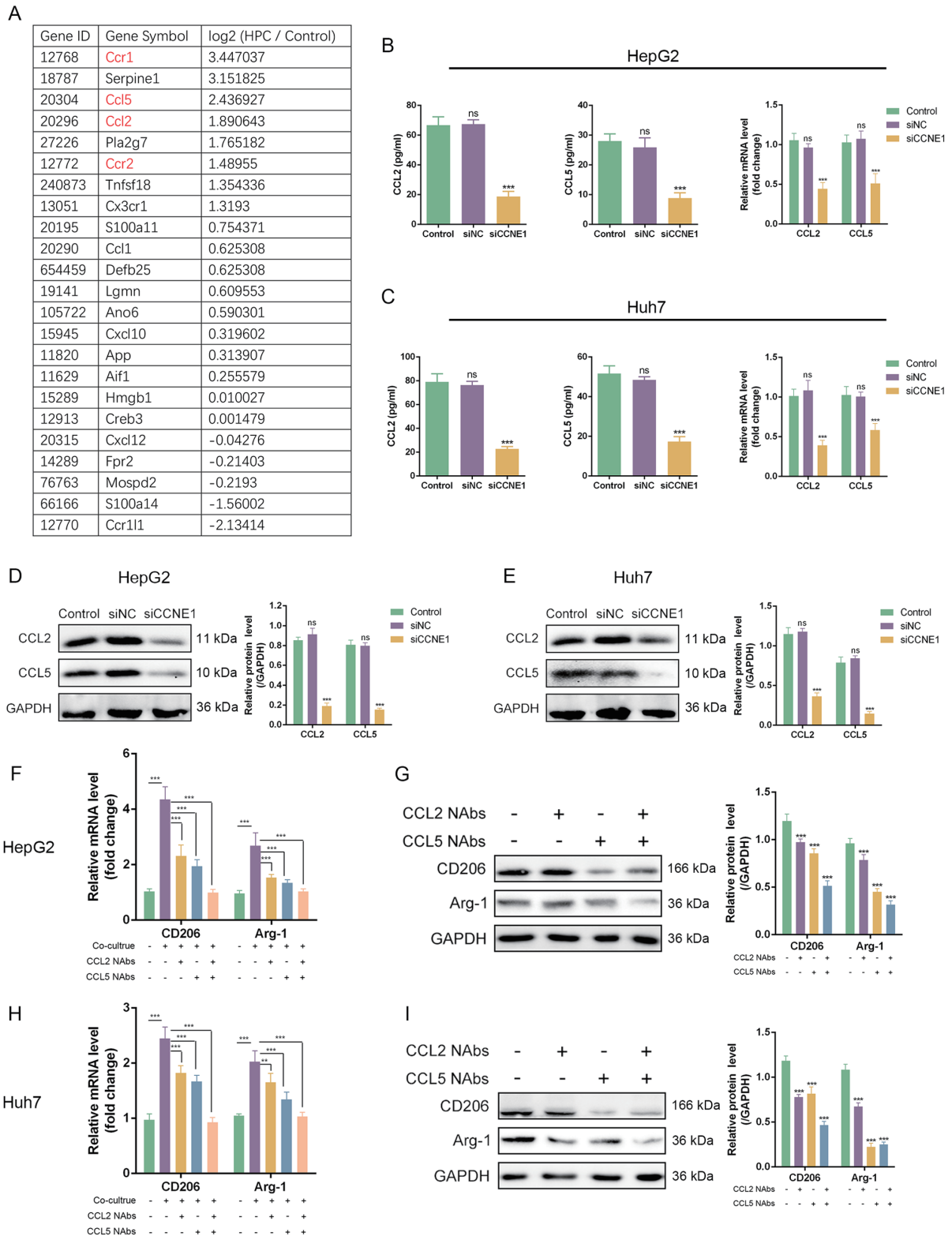


**Fig. 7. Mechanism of CCNE1-induced TAM polarization.** (A) Enrichment of CCR1, CCL5, CCL2, and CCR2 in the “monocyte chemotaxis” pathway. (B) ELISA and RT-qPCR were used to detect the levels of CCL2 and CCL5 in HepG2 cells. (C) ELISA and RT-qPCR were used to detect the levels of CCL2 and CCL5 in Huh7 cells. (D-E) The protein levels of CCL2 and CCL5 in HepG2 and Huh7 cells. (F) The mRNA levels of CD206 and Arg-1. (G) The protein levels of CD206 and Arg-1. (H) The mRNA levels of CD206 and Arg-1. (I) The protein levels of CD206 and Arg-1. ns, not significant; \*\* $p < 0.01$ ; \*\*\* $p < 0.001$ . CCNE1, Cyclin E1; CCL2, Chemokine (C-C motif) ligand 2; CCL5, Chemokine (C-C motif) ligand 5; Nabs, neutralizing antibody; Arg-1, Arginase-1; GAPDH, glyceraldehyde 3-phosphate dehydrogenase; +, with; -, without.

E-type cyclins are key components of the cell cycle machinery that regulate various physiological and pathological processes.<sup>8</sup> CCNE1, the first identified E-type cyclin, activates CDK2 kinase, inducing entry into the S phase.<sup>26</sup> The normal activity of the CCNE1/CDK2 complex is essential for proper cell cycle progression and DNA replication. Its oncogenic activation has been shown to interfere with DNA replication, causing replication stress through various mechanisms and leading to genomic instability in human cancers.<sup>27</sup> CCNE1 is overexpressed or amplified in many human cancers, contributing to resistance against standard treatments and targeted chemotherapeutic agents, and is associated with poor clinical outcomes and reduced survival.<sup>28,29</sup> A study by Sonntag *et al.*<sup>30</sup> showed that while CCNE1 and CDK2 are essential for HCC development, HCC progression is regulated by mechanisms independent of CDK2 activity, and genetic inactivation of CCNE1 prevents HCC development in mice. However, the individual contribution and mechanism of CCNE1 in HPC-to-HCC progression remain incompletely understood. In this study, CCNE1 expression was significantly upregulated in HPC mice, overexpressed in human dysplastic nodules and HCC samples, and correlated with poor survival in patients. In addition, CCNE1 was minimally expressed in normal hepatocytes but highly expressed in HCC cells. Silencing CCNE1 significantly inhibited HCC cell proliferation, migration, and invasion, and increased apoptosis. These findings suggest that CCNE1 overexpression promotes the malignant phenotype and early progression of HCC.

RNA sequencing analysis revealed that CCNE1 activates the PI3K/Akt signaling pathway in the liver tissues of HPC mice. This pathway is a critical regulator of cell proliferation, growth, metabolism, and motility. In human cancers, genetic alterations in this pathway are frequent, and its components represent important molecular targets for therapy.<sup>31,32</sup> *In vitro* experiments confirmed that CCNE1 promoted HCC cell proliferation, migration, invasion, and survival via PI3K/Akt activation. This mechanistic link offers actionable targets for therapeutic development in HCC. Pharmacological inhibition of the PI3K/Akt pathway effectively reversed CCNE1-driven malignant phenotypes in HCC cells, suggesting that combining CCNE1-targeted agents with existing kinase inhibitors may enhance therapeutic efficacy.

In recent years, immune cell therapy has shown remarkable efficacy in cancer treatment. However, immunosuppressive cells in the TME limit its clinical benefits. In particular, the crosstalk between cancer cells and TAMs allows cancer cells to evade immune defenses and facilitates cancer progression.<sup>33</sup> Li and colleagues showed that NLRP7 promotes colorectal cancer progression by inducing TAM recruitment and pro-tumor M2-like macrophage polarization.<sup>34</sup> A study by Xu *et al.*<sup>35</sup> proved that abundant M2 TAMs in HER2/neu<sup>+</sup> breast tumors represent a barrier to anti-HER2/neu antibody therapy. In the present study, immunohistochemical analysis showed increased macrophage infiltration and VEGF expression in the liver tissues of HPC mice. Furthermore, *in vitro* coculture experiments revealed that CCNE1 overexpression in HCC cells promotes macrophage polarization toward the M2 phenotype, partially enhancing its carcinogenic effect. TAMs exhibit plasticity, and their functional roles are regulated by molecules in the TME.<sup>36</sup> Chemokines are central mediators of the crosstalk between tumor cells and TAMs, coordinating TAM recruitment and polarization.<sup>37</sup> Colony-stimulating factor-1 (CSF1) and CSF1 receptor are critical ligand-receptor pairs involved in macrophage differentiation and survival. Several studies have shown that blocking CSF1 or its receptor can repolarize TAMs from the M2 to the M1 phenotype

and increase cancer cell sensitivity to immunotherapies, such as PD-L1 blockade.<sup>38,39</sup> Our data revealed that CCNE1 induces M2 polarization of TAMs via CCL2/CCL5 secretion, thereby fostering an immunosuppressive TME. This suggests that neutralizing CCL2/CCL5 with monoclonal antibodies or CCR5 antagonists could reverse TAM polarization and work synergistically with immune checkpoint inhibitors (ICIs) such as anti-PD-1/PD-L1 antibodies. This combination strategy could enhance T-cell infiltration and help overcome ICI resistance in HCC.

In this study, the *in vitro* experiments primarily utilized HepG2 and Huh7 cell lines. It is important to note that the origin of HepG2 remains controversial, as it has been suggested to derive from hepatoblastoma rather than HCC.<sup>40</sup> However, HepG2 remains widely employed in HCC research due to its established utility in modeling hepatocellular carcinogenesis.<sup>41,42</sup> Importantly, the experimental results from Huh7 cells confirmed the functional role of CCNE1 in HCC progression. Future studies will incorporate additional validated HCC cell lines to further corroborate these findings.

## Conclusions

This study identifies CCNE1 as a pivotal driver of HPC-to-HCC progression, playing multifaceted roles in tumor cell survival, invasion, and immune evasion. Its expression is positively correlated with early vascular invasion and late distant metastasis in HCC. Mechanistically, CCNE1 promotes tumorigenesis via PI3K/Akt pathway activation and fosters an immunosuppressive microenvironment through CCL2/CCL5-mediated TAM infiltration and M2 polarization. These findings highlight CCNE1 as a promising biomarker for early HCC diagnosis and a potential therapeutic target for disrupting both tumor-intrinsic signaling and the immunosuppressive microenvironment. However, several limitations must be acknowledged. First, although our bioinformatic analyses of TCGA and GEO datasets validate CCNE1's clinical relevance, prospective studies with longitudinal HPC-to-HCC cohorts are needed to confirm its predictive value. Second, the functional crosstalk between CCNE1 and other signaling pathways or molecules remains unexplored. Finally, preclinical models (e.g., CCNE1-transgenic mice) are essential to validate its causal role in HPC progression and to evaluate targeted therapies *in vivo*. Future studies should confirm these findings in longitudinal cohorts and preclinical models to translate CCNE1's diagnostic and therapeutic potential into clinical practice. By bridging mechanistic insights with clinical needs, this work lays the foundation for precision medicine strategies to intercept HCC at its precancerous stage.

## Funding

None to declare.

## Conflict of interest

The authors have no conflict of interests related to this publication.

## Author contributions

Study concept (WG), study design (WG, KZ, XH, LY), experiment performance, data acquisition, data analysis (KZ, XH, LY), drafting of the manuscript (KZ), and revision of the manuscript (WG). All authors contributed to the article and approved the final version.

**Ethical statement**

All animal experiments were approved by the Animal Care and Use Committee of The First Affiliated Hospital of Zhengzhou University (No. 2019-KY-21). All animals received human care.

**Data sharing statement**

The datasets generated for this study are available from the corresponding author upon reasonable request.

**References**

[1] Ferlay J, Soerjomataram I, Dikshit R, Eser S, Mathers C, Rebelo M, *et al*. Cancer incidence and mortality worldwide: sources, methods and major patterns in GLOBOCAN 2012. *Int J Cancer* 2015;136(5):E359–E386. doi:10.1002/ijc.29210, PMID:25220842.

[2] Nam SW, Park JY, Ramasamy A, Shevade S, Islam A, Long PM, *et al*. Molecular changes from dysplastic nodule to hepatocellular carcinoma through gene expression profiling. *Hepatology* 2005;42(4):809–818. doi:10.1002/hep.20878, PMID:16175600.

[3] Ostrand-Rosenberg S. Tolerance and immune suppression in the tumor microenvironment. *Cell Immunol* 2016;299:23–29. doi:10.1016/j.cellimm.2015.09.011, PMID:26435343.

[4] Binnewies M, Roberts EW, Kersten K, Chan V, Fearon DF, Merad M, *et al*. Understanding the tumor immune microenvironment (TIME) for effective therapy. *Nat Med* 2018;24(5):541–550. doi:10.1038/s41591-018-0014-x, PMID:29686425.

[5] Li X, Liu R, Su X, Pan Y, Han X, Shao C, *et al*. Harnessing tumor-associated macrophages as aids for cancer immunotherapy. *Mol Cancer* 2019;18(1):177. doi:10.1186/s12943-019-1102-3, PMID:31805946.

[6] Anfray C, Umbarino A, Andón FT, Allavena P. Current Strategies to Target Tumor-Associated-Macrophages to Improve Anti-Tumor Immune Responses. *Cells* 2019;9(1):46. doi:10.3390/cells9010046, PMID:31878087.

[7] Mantovani A, Marchesi F, Malesci A, Laghi L, Allavena P. Tumour-associated macrophages as treatment targets in oncology. *Nat Rev Clin Oncol* 2017;14(7):399–416. doi:10.1038/nrclinonc.2016.217, PMID:28117416.

[8] Chu C, Geng Y, Zhou Y, Scicinski P. Cyclin E in normal physiology and disease states. *Trends Cell Biol* 2021;31(9):732–746. doi:10.1016/j.tcb.2021.05.001, PMID:34052101.

[9] Alsina M, Landolfi S, Aura C, Caci K, Jimenez J, Prudkin L, *et al*. Cyclin E amplification/overexpression is associated with poor prognosis in gastric cancer. *Ann Oncol* 2015;26(2):438–439. doi:10.1093/annonc/mdu535, PMID:25403579.

[10] Nakayama K, Rahman MT, Rahman M, Nakamura K, Ishikawa M, Katagiri H, *et al*. CCNE1 amplification is associated with aggressive potential in endometrioid endometrial carcinomas. *Int J Oncol* 2016;48(2):506–516. doi:10.3892/ijo.2015.3268, PMID:26647729.

[11] Xu H, George E, Kinose Y, Kim H, Shah JB, Peake JD, *et al*. CCNE1 copy number is a biomarker for response to combination WEE1-ATR inhibition in ovarian and endometrial cancer models. *Cell Rep Med* 2021;2(9):100394. doi:10.1016/j.xcrm.2021.100394, PMID:34622231.

[12] Turner NC, Liu Y, Zhu Z, Loi S, Colleonì M, Loibl S, *et al*. Cyclin E1 Expression and Palbociclib Efficacy in Previously Treated Hormone Receptor-Positive Metastatic Breast Cancer. *J Clin Oncol* 2019;37(14):1169–1178. doi:10.1200/JCO.18.00925, PMID:30807234.

[13] Hwang HC, Clurman BE. Cyclin E in normal and neoplastic cell cycles. *Oncogene* 2005;24(17):2776–2786. doi:10.1038/sj.onc.1208613, PMID:15838514.

[14] Karst AM, Jones PM, Vena N, Ligon AH, Liu JF, Hirsch MS, *et al*. Cyclin E1 deregulation occurs early in secretory cell transformation to promote formation of fallopian tube-derived high-grade serous ovarian cancers. *Cancer Res* 2014;74(4):1141–1152. doi:10.1158/0008-5472.CAN-13-2247, PMID:24366882.

[15] Geng Y, Michowski W, Chick JM, Wang YE, Jecrois ME, Sweeney KE, *et al*. Kinase-independent function of E-type cyclins in liver cancer. *Proc Natl Acad Sci U S A* 2018;115(5):1015–1020. doi:10.1073/pnas.1711477115, PMID:29339491.

[16] Sahraeian SME, Mohiyuddin M, Sebra R, Tilgner H, Afshar PT, Au KF, *et al*. Gaining comprehensive biological insight into the transcriptome by performing a broad-spectrum RNA-seq analysis. *Nat Commun* 2017;8(1):59. doi:10.1038/s41467-017-00050-4, PMID:28680106.

[17] Yao L, Hu X, Yuan M, Zhang Q, Liu P, Yang L, *et al*. IGF2-NR4A2 Signaling Regulates Macrophage Subtypes to Attenuate Liver Cirrhosis. *J Clin Transl Hepatol* 2023;11(4):787–799. doi:10.14218/JCTH.2022.00392, PMID:37408817.

[18] Yu A, Zhao L, Kang Q, Li J, Chen K, Fu H. Transcription factor HIF1 $\alpha$  promotes proliferation, migration, and invasion of cholangiocarcinoma via long noncoding RNA H19/microRNA-612/Bcl-2 axis. *Transl Res* 2020;224:26–39. doi:10.1016/j.trsl.2020.05.010, PMID:32505707.

[19] Lou Y, Lu J, Zhang Y, Gu P, Wang H, Qian F, *et al*. The centromere-associated

ed protein CENPU promotes cell proliferation, migration, and invasiveness in lung adenocarcinoma. *Cancer Lett* 2022;532:215599. doi:10.1016/j.canlet.2022.215599, PMID:35176420.

[20] He Y, Sun MM, Zhang GG, Yang J, Chen KS, Xu WW, *et al*. Targeting PI3K/Akt signal transduction for cancer therapy. *Signal Transduct Target Ther* 2021;6(1):425. doi:10.1038/s41392-021-00828-5, PMID:34916492.

[21] Wang YC, Wang X, Yu J, Ma F, Li Z, Zhou Y, *et al*. Targeting monoamine oxidase A-regulated tumor-associated macrophage polarization for cancer immunotherapy. *Nat Commun* 2021;12(1):3530. doi:10.1038/s41467-021-23164-2, PMID:34112755.

[22] Komohara Y, Takeya M. CAFs and TAMs: maestros of the tumour microenvironment. *J Pathol* 2017;241(3):313–315. doi:10.1002/path.4824, PMID:27753093.

[23] Kraus S, Kolman T, Yeung A, Deming D. Chemokine Receptor Antagonists: Role in Oncology. *Curr Oncol Rep* 2021;23(11):131. doi:10.1007/s11912-021-01117-8, PMID:34480662.

[24] Bule P, Aguiar SI, Aires-Da-Silva F, Dias JNR. Chemokine-Directed Tumor Microenvironment Modulation in Cancer Immunotherapy. *Int J Mol Sci* 2021;22(18):9804. doi:10.3390/ijms22189804, PMID:34575965.

[25] Yang Y, Lin X, Lu X, Luo G, Zeng T, Tang J, *et al*. Interferon-microRNA signalling drives liver precancerous lesion formation and hepatocarcinogenesis. *Gut* 2016;65(7):1186–1201. doi:10.1136/gutjnl-2015-310318, PMID:26860770.

[26] Kanska J, Zakhour M, Taylor-Harding B, Karlan BY, Wiedemeyer WR. Cyclin E as a potential therapeutic target in high grade serous ovarian cancer. *Gynecol Oncol* 2016;143(1):152–158. doi:10.1016/j.ygyno.2016.07.111, PMID:27461360.

[27] Fagundes R, Teixeira LK. Cyclin E/CDK2: DNA Replication, Replication Stress and Genomic Instability. *Front Cell Dev Biol* 2021;9:774845. doi:10.3389/fcell.2021.774845, PMID:34901021.

[28] Suski JM, Braun M, Strmiska V, Scicinski P. Targeting cell-cycle machinery in cancer. *Cancer Cell* 2021;39(6):759–778. doi:10.1016/j.ccell.2021.03.010, PMID:33891890.

[29] Schraml P, Bucher C, Bissig H, Nocito A, Haas P, Wilber K, *et al*. Cyclin E overexpression and amplification in human tumours. *J Pathol* 2003;200(3):375–382. doi:10.1002/path.1356, PMID:12845634.

[30] Sonntag R, Giebler N, Nevzorova YA, Bangen JM, Fahrenkamp D, Lambert D, *et al*. Cyclin E1 and cyclin-dependent kinase 2 are critical for initiation, but not for progression of hepatocellular carcinoma. *Proc Natl Acad Sci U S A* 2018;115(37):9282–9287. doi:10.1073/pnas.1807155115, PMID:30150405.

[31] Alzahrani AS. PI3K/Akt/mTOR inhibitors in cancer: At the bench and bedside. *Semin Cancer Biol* 2019;59:125–132. doi:10.1016/j.semcancer.2019.07.009, PMID:31323288.

[32] Fresno Vara JA, Casado E, de Castro J, Cejas P, Belda-Iniesta C, González-Barón M. PI3K/Akt signalling pathway and cancer. *Cancer Treat Rev* 2004;30(2):193–204. doi:10.1016/j.ctrv.2003.07.007, PMID:15023437.

[33] Anderson NR, Minutolo NG, Gill S, Klichinsky M. Macrophage-Based Approaches for Cancer Immunotherapy. *Cancer Res* 2021;81(5):1201–1208. doi:10.1158/0008-5472.CAN-20-2990, PMID:33203697.

[34] Li B, Qi ZP, He DL, Chen ZH, Liu JY, Wong MW, *et al*. NLRP7 deubiquitination by USP10 promotes tumor progression and tumor-associated macrophage polarization in colorectal cancer. *J Exp Clin Cancer Res* 2021;40(1):126. doi:10.1186/s13046-021-01920-y, PMID:33838681.

[35] Xu M, Liu M, Du X, Li S, Li H, Li X, *et al*. Intratumoral Delivery of IL-21 Overcomes Anti-Her2/Neu Resistance through Shifting Tumor-Associated Macrophages from M2 to M1 Phenotype. *J Immunol* 2015;194(10):4997–5006. doi:10.4049/jimmunol.1402603, PMID:25876763.

[36] Pan Y, Yu Y, Wang X, Zhang T. Tumor-Associated Macrophages in Tumor Immunity. *Front Immunol* 2020;11:583084. doi:10.3389/fimmu.2020.583084, PMID:33365025.

[37] Qin R, Ren W, Ya G, Wang B, He J, Ren S, *et al*. Role of chemokines in the crosstalk between tumor and tumor-associated macrophages. *Clin Exp Med* 2023;23(5):1359–1373. doi:10.1007/s10238-022-00888-z, PMID:36173487.

[38] Pyonteck SM, Akkari L, Schuhmacher AJ, Bowman RL, Sevenich L, Quail DF, *et al*. CSF-1R inhibition alters macrophage polarization and blocks glioma progression. *Nat Med* 2013;19(10):1264–1272. doi:10.1038/nm.3337, PMID:24056773.

[39] Zhu Y, Yang J, Xu D, Gao XM, Zhang Z, Hsu JL, *et al*. Disruption of tumour-associated macrophage trafficking by the osteopontin-induced colony-stimulating factor-1 signalling sensitises hepatocellular carcinoma to anti-PD-L1 blockade. *Gut* 2019;68(9):1653–1666. doi:10.1136/gutjnl-2019-318419, PMID:30902885.

[40] López-Terrada D, Cheung SW, Finegold MJ, Knowles BB. Hep G2 is a hepatoblastoma-derived cell line. *Hum Pathol* 2009;40(10):1512–1515. doi:10.1016/j.humpath.2009.07.003, PMID:19751877.

[41] Zhao B, Liang Z, Zhang L, Jiang L, Xu Y, Zhang Y, *et al*. Ponicidin Promotes Hepatocellular Carcinoma Mitochondrial Apoptosis by Stabilizing Keap1-PGAM5 Complex. *Adv Sci (Weinh)* 2024;11(38):e2406080. doi:10.1002/advs.202406080, PMID:39116422.

[42] Yao J, Tang S, Shi C, Lin Y, Ge L, Chen Q, *et al*. Isoginkgetin, a potential CDK6 inhibitor, suppresses SLC2A1/GLUT1 enhancer activity to induce AMPK-ULK1-mediated cytotoxic autophagy in hepatocellular carcinoma. *Autophagy* 2023;19(4):1221–1238. doi:10.1080/15548627.2022.2119353, PMID:36048765.